

Luminescence kinetics of $\text{Y}_{0.8}\text{Yb}_{0.2}\text{F}_3:\text{Tm}^{3+}$ solid solution crystal

V. V. Pavlov¹, B. N. Kazakov, A. V. Lovchev

Kazan (Volga Region) Federal University, 420008 Kazan, Russia

Submitted 26 May 2014

Resubmitted 9 June 2014

Upconversion luminescence kinetics of Tm^{3+} doped $\text{Y}_{0.8}\text{Yb}_{0.2}\text{F}_3$ solid solution crystal was studied for various values of pulse excitation parameters: pulse duration, wavelength and excitation power. Analysis of obtained results allowed to make a conclusion about the presence of transient processes. The transient processes found in upconversion luminescence kinetics are characterized by duration commensurate with lifetime of the excited energy levels of the activator ions. Upon completion of these processes a stable equilibrium state is established between the processes of population and spontaneous decay of the excited energy levels of Tm^{3+} ions. Conditions under which the equilibrium state can be maintained have been considered.

DOI: 10.7868/S0370274X14130037

1. Introduction. Rare earth double-doped micro- and nanocrystals due to efficient transformation of infrared (IR) radiation into visible and ultraviolet (UV) luminescence have found wide application, for example in color displays, solar panels, IR indicators [1, 2]. When designing such devices a system with high efficiency of energy transformation is required. It is also important to know the characteristics of transient processes (a transient response), which determine the steady-state conditions of their operation. The transient response can be determined using different external actions (impulse and step responses). Impulse responses are studied under excitation of a sample by impulse radiation with the pulse duration of the order of a nanosecond or less. Application of excitation in the form of rectangular pulses with the pulse duration more than the duration of the transient processes enables to investigate step responses of a system.

In this work we report the results of investigation of the impulse and step responses of upconversion (UC) luminescence kinetics of Tm^{3+} doped $\text{Y}_{0.8}\text{Yb}_{0.2}\text{F}_3$ solid solution crystal. The aim of investigation is to determine the conditions under which in the crystal a stable equilibrium state may be established between the processes of population and spontaneous decay of the excited energy levels of Tm^{3+} ions.

The choice of investigated crystal is due to the fact that in $\text{YF}_3:\text{Yb}^{3+},\text{Tm}^{3+}$ nanoparticles an effective energy transfer between Yb^{3+} and Tm^{3+} ions, that leads to the intensive UC-luminescence of Tm^{3+} ions, has been observed [3, 4]. It is known that efficiency of en-

ergy transfer between rare earth activator ions strongly depends on the size and structure of nanocrystals [5, 6]. For example, the intensity of UV UC-luminescence of Tm^{3+} ions dramatically increases with decrease of the size of $\text{YF}_3:\text{Yb}^{3+},\text{Tm}^{3+}$ nanoparticles [3, 4]. In our work we study the macroscopic sample $\text{Y}_{0.8}\text{Yb}_{0.2}\text{F}_3:\text{Tm}^{3+}$ and therefore the results of our UC-luminescence investigation are not influenced by such effects.

2. Experimental details. The $\text{Y}_{0.8}\text{Yb}_{0.2}\text{F}_3:\text{Tm}^{3+}$ solid solution crystal was synthesized by the Bridgman technique in graphite crucible under extra pure argon atmosphere. Additional fluorination of the atmosphere was obtained through pyrolysis of tetrafluoroethylene. The concentration of Tm^{3+} impurity ions was 1 at.% in the melt. Since YF_3 and YbF_3 have several polymorphic transitions near melting point the crystal has grown in the form of transparent needle or plate with small dimensions ($\sim 1 \times 15 \text{ mm}^2$). X-ray structural analysis has proved that the crystal is single-phase with orthorhombic system (space group Pnma (D_{2h}^{16}) with point symmetry of Cs rare earth impurity center).

Luminescence spectra were registered by StellarNet spectrometer, which detects luminescence signal in the 200–1100 nm spectral range with a spectral resolution of 0.5 nm. Luminescence kinetics was recorded using the optical spectrometer based on prismatic monochromator ZMR-3 (glass prism, spectral resolution $\sim 0.2\text{--}0.5 \text{ nm}$), FEU-79 photomultiplier and high-speed 4 channel A/D conversion module L-Card E20-10.

For luminescence excitation the third and second harmonics of the $\text{Al}_2\text{O}_3:\text{Ti}$ laser (240–280 and 350–700 nm, 10 Hz, 10 ns), the optical parametric oscillator laser system (420–1200 nm, 10 Hz, 10 ns) (OPO) and in-

¹)e-mail: Vitaly.V.Pavlov@gmail.com

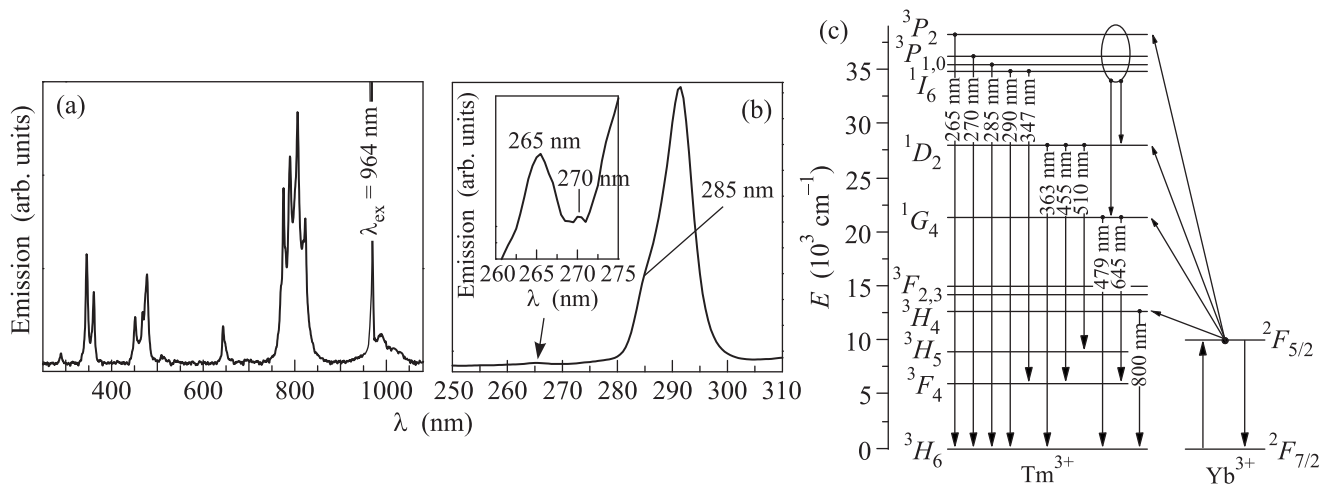


Fig. 1. – Room-temperature luminescence spectrum of $\text{Y}_{0.8}\text{Yb}_{0.2}\text{F}_3:\text{Tm}^{3+}$ crystal under IR LD excitation ($\lambda_{\text{ex}} = 964$ nm, $P_{\text{LD}} = 400$ mW), registered in 250–1080 nm (a) and 250–310 nm (b) spectral ranges. (c) – The energy level diagram of Yb^{3+} and Tm^{3+} ions and possible upconversion processes in $\text{YF}_3:\text{Yb}^{3+}, \text{Tm}^{3+}$ crystal

frared semiconductor laser (920–980 nm) (IR laser diode or IR LD) were used. When studying luminescence kinetics the IR LD radiation was modulated in such a way as to the temporal behavior of radiation represented a sequence of rectangular pulses with modulation frequency $f_{\text{mod}} = 66.7$ Hz and pulse duration $t_{\text{ex}} = (0.2\text{--}14)$ ms. All experiments were carried out at 300 K.

3. Experimental results. 3.1. Luminescence spectra. Irradiation of the sample, which is resonant with the $4f\text{--}4f$ transitions of Yb^{3+} ions, excites not only emission of Yb^{3+} ions but also intensive luminescence of Tm^{3+} ions. The luminescence spectrum in the 250–1080 nm spectral range obtained under excitation of the sample at 964 nm (IR LD radiation) is shown in Fig. 1a and b. In near-IR region of this spectrum ($\lambda_{\text{em}} = (930\text{--}1080)$ nm) the luminescence of Yb^{3+} ions is observed (${}^2F_{5/2} \rightarrow {}^2F_{7/2}$). Radiative transitions of Tm^{3+} ions under excitation at 964 nm as a result of upconversion processes are shown by arrows in Fig. 1c. Suggested in [7] possible upconversion processes are also shown in Fig. 1c.

Changing the excitation wavelength in the 920–980 nm spectral range (IR LD radiation) results only in change of the integral intensity of luminescence of Tm^{3+} and Yb^{3+} ions. Its maximum is observed under excitation at 980 nm. With increase of the power of IR LD excitation radiation the integral intensity of all luminescence lines of Tm^{3+} and Yb^{3+} ions also increases. This allowed us to detect the weak luminescence lines in the UV spectral range corresponding to the ${}^3P_j \rightarrow {}^3H_6$ transitions of Tm^{3+} ions (Fig. 1b).

The intensities of luminescence lines with $\lambda_{\text{em}} = 347$ nm (${}^1I_6 \rightarrow {}^3F_4$) and 363 nm (${}^1D_2 \rightarrow {}^3H_6$) of Tm^{3+} ions depend on the excitation power in different ways (Fig. 2a). Similar changes in the power dependence of UV UC-luminescence spectra were observed for $\text{NaYF}_4:\text{Yb}^{3+}, \text{Tm}^{3+}$ nanocrystals [8]. We suggested that several mechanisms are involved in population of the excited energy levels of Tm^{3+} ions and their contribution varies in different excitation power ranges. One of the mechanisms is determined by the transitions from the 3P_j and 1I_6 excited energy levels to the lower levels of Tm^{3+} ions as shown in Fig. 1c.

Thereby, the effective energy transfer takes place in $\text{Y}_{0.8}\text{Yb}_{0.2}\text{F}_3:\text{Tm}^{3+}$ solid solution crystal from Yb^{3+} ions to Tm^{3+} ions. We also detected energy transfer from Tm^{3+} ions to Yb^{3+} ions (down-conversion) under excitation of the sample at the wavelengths corresponding to the $4f\text{--}4f$ transitions of Tm^{3+} ions ($\lambda_{\text{ex}} = 355, 464, 680$ nm; ${}^3H_6 \rightarrow {}^1D_2, {}^1G_4,$ and 3F_3). As an example, the luminescence spectrum under excitation at $\lambda_{\text{ex}} = 464$ nm, in which there is luminescence of both Tm^{3+} and Yb^{3+} ions, is shown in Fig. 2c.

3.2. Luminescence kinetics. Dynamics of the energy transfer from excited subsystem to unexcited one manifests itself in luminescence kinetics. In most works UC-luminescence kinetics in rare earth double-doped nanocrystals was studied under excitation by nanosecond pulses with the repetition rate of 10 Hz and only impulse response was investigated [3, 7, 9].

We also started our study of luminescence kinetics with excitation by nanosecond pulse. The luminescence curve of Tm^{3+} ions in $\text{Y}_{0.8}\text{Yb}_{0.2}\text{F}_3:\text{Tm}^{3+}$ solid solu-

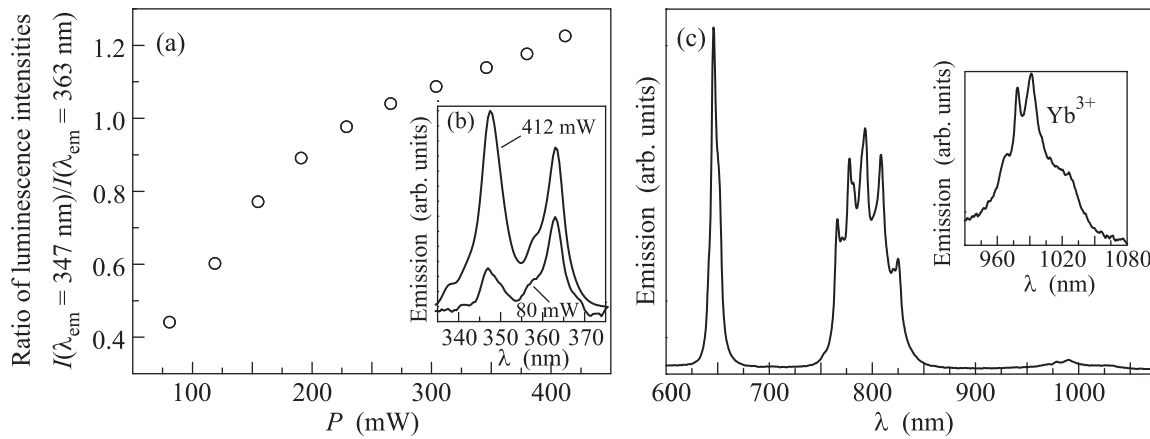


Fig. 2. (a) – Ratio of intensities of the Tm^{3+} luminescence lines with $\lambda_{em} = 347$ nm (${}^1I_6 \rightarrow {}^3F_4$) and $\lambda_{em} = 363$ nm (${}^1D_2 \rightarrow {}^3H_6$) as a function of power of excitation radiation at 933 nm ($T = 300$ K). (b)– Room-temperature luminescence spectra for two different values of excitation power 80 and 412 mW ($\lambda_{ex} = 933$ nm). (c) – Room-temperature luminescence spectrum of $Y_{0.8}Yb_{0.2}F_3:Tm^{3+}$ crystal under excitation by OPO laser system at 464 nm, registered in 600–1080 nm spectral range

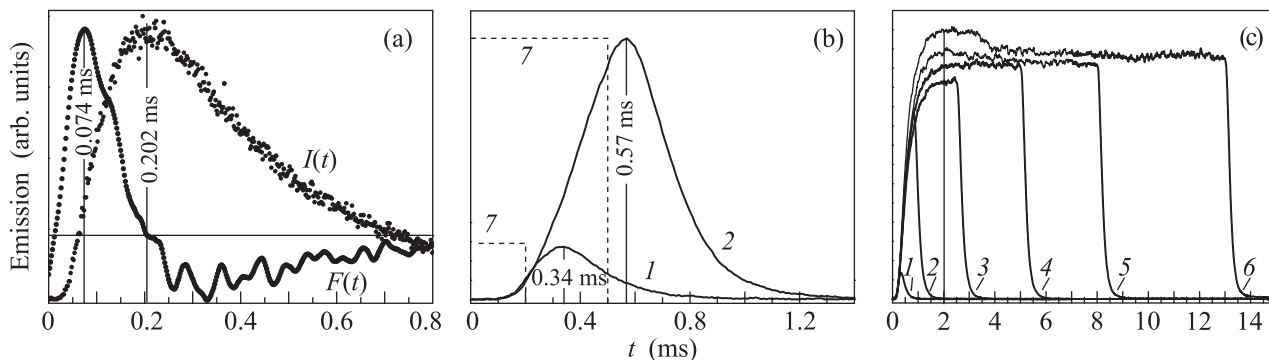


Fig. 3. (a)– Time dependences of UC-luminescence intensity $I(t)$ and its first derivative $F(t)$ in $Y_{0.8}Yb_{0.2}F_3:Tm^{3+}$ crystal under excitation by OPO laser system at 980 nm ($\lambda_{em} = 479$ nm, $T = 300$ K). (b, c) – Time evolution of UC-luminescence intensity of $Y_{0.8}Yb_{0.2}F_3:Tm^{3+}$ crystal under IR LD excitation with the pulse durations of 0.2 ms (1), 0.5 ms (2), 2.5 ms (3), 5 ms (4), 8 ms (5), 13 ms (6). Excitation pulses are shown by dotted lines 7 ($\lambda_{ex} = 933$ nm, $\lambda_{em} = 363$ nm, $P_{LD} = 400$ mW, $T = 300$ K)

tion crystal under excitation by OPO laser system at the wavelength 980 nm ($\lambda_{em} = 479$ nm, $t_{ex} = 10$ ns) is shown in Fig. 3a. The $\lambda_{em} = 479$ nm radiation corresponds to the ${}^1G_4 \rightarrow {}^3H_6$ transition of Tm^{3+} ions. The luminescence kinetics has a maximum at $t = 0.2$ ms, which corresponds to the short-term state of dynamic equilibrium between two nonequilibrium processes of population and decay of the excited 1G_4 energy level. The rise of luminescence curve shows that population of the excited level goes with varying acceleration. The point of time at which luminescence rise slows down may be determined from analysis of the first derivative of luminescence: $F(t) = dI(t)/dt$.

This dependence $F(t)$ has a maximum at $t = 0.074$ ms which corresponds to the point of time when the rate of luminescence rise starts decreasing. Also, the

dependence $F(t)$ shows the points of inflexion, that indicate the presence of several processes of population of the excited 1G_4 level (Fig. 3a). It confirms the result obtained from analysis of the dependence of luminescence intensity, corresponding to the ${}^1I_6 \rightarrow {}^3F_4$ and ${}^1D_2 \rightarrow {}^3H_6$ transitions of Tm^{3+} ions, on the excitation power (Fig. 2a). The luminescence decay of the ${}^1G_4 \rightarrow {}^3H_6$ transition is characterized by the decay time of about 0.33 ms.

However the study of step response and steady-state response requires the excitation pulse duration significantly exceeding that of transient processes. Therefore the luminescence kinetics of $Y_{0.8}Yb_{0.2}F_3:Tm^{3+}$ crystal was studied under rectangular pulse excitation with the duration of 0.2–14 ms and modulation frequency $f_{mod} = 66.7$ Hz. The luminescence kinetics of Tm^{3+}

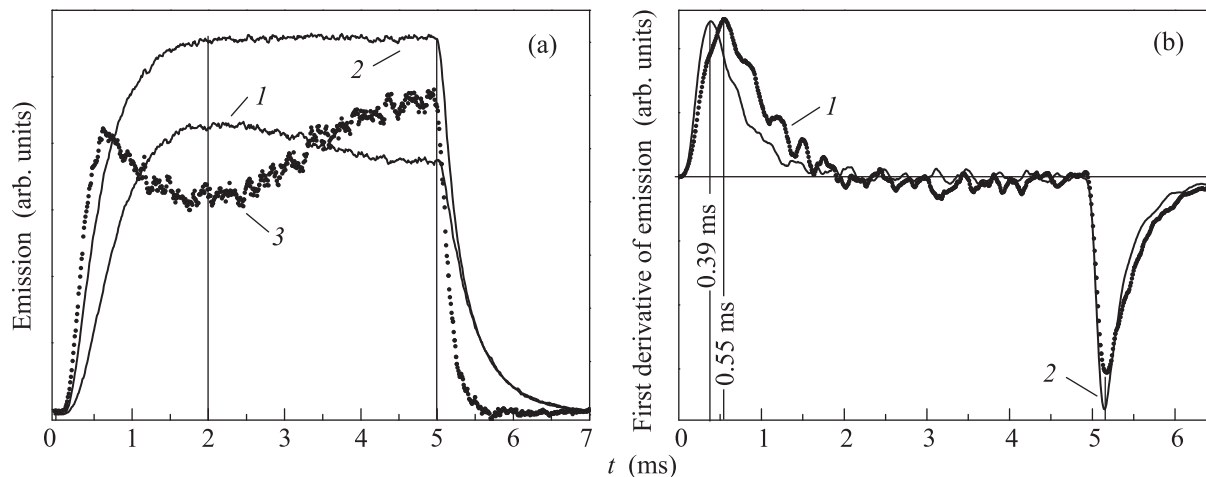


Fig. 4. (a) – Time evolution of UC-luminescence intensity of $Y_{0.8}Yb_{0.2}F_3:Tm^{3+}$ crystal under IR LD excitation with excitation power of 150 mW (1) and 400 mW (2) and difference between these luminescence kinetics ($I_2 - I_1$) (3). (b) – Time dependence of the first derivative of Tm^{3+} luminescence intensity, registered for 150 mW (1), 400 mW (2) excitation powers ($\lambda_{ex} = 933$ nm, $\lambda_{em} = 479$ nm, $T_{ex} = 15$ ms, $t_{ex} = 5$ ms, $T = 300$ K)

ions was excited at the 920–980 nm spectral range. Time evolution of luminescence intensity was registered for the following radiative transitions of Tm^{3+} ions: $^1D_2 \rightarrow ^3H_6$ (363 nm), $^1D_2 \rightarrow ^3F_4$ (454 nm), $^1D_2 \rightarrow ^3H_5$ (512 nm), $^1G_4 \rightarrow ^3H_6$ (464, 479 nm), $^1G_4 \rightarrow ^3F_4$ (646 nm).

A number of common regularities were revealed in the luminescence kinetics for all wavelengths of excitation and luminescence.

1. The temporal behavior of luminescence intensity depends on the excitation pulse duration. Upon the end of excitation pulse with the duration $t_{ex} = (0.2-0.8)$ ms the luminescence intensity continues rising for some time until it reaches its maximum (Fig. 3b). When the pulse duration of excitation takes on values 0.8–2.0 ms, the intensity of luminescence reaches its maximum value at the end of the excitation pulse. When the pulse duration of excitation is greater than 2.5 ms, the location of maximum of the luminescence intensity does not vary with the pulse duration of excitation and is equal to about 2 ms (Fig. 3c). If the pulse duration of excitation is 2.5–14 ms, after the maximum of luminescence there is either a monotonic decrease of luminescence $I_1(t)$ for the excitation power of about 150 mW or a plateau $I_2(t)$ for the excitation power of about 400 mW (Fig. 4a). The plateau of luminescence curve characterizes the state of dynamic equilibrium between the processes of population and spontaneous decay of the excited energy levels of Tm^{3+} ions.

2. The rates of luminescence rise at the start of excitation pulse and its decay upon the end of the excitation pulse depend on the excitation power (Fig. 4a). It be-

comes apparent in temporal behavior of the first derivative of luminescence. For example, comparison of the first derivatives of dependences $I_1(t)$ and $I_2(t)$ demonstrates that the increase of the excitation power leads to the shift of maximum of the first derivative towards the start of excitation pulse (Fig. 4b). As time dependence of the first derivative of luminescence has several points of inflexion it may be concluded that the luminescence kinetics includes information about several processes with different rates of luminescence rise and decay. The relative contribution of high-frequency processes to the luminescence kinetics increases with increase of excitation power (Fig. 4b).

4. Summary. The luminescence spectra of Tm^{3+} doped $Y_{0.8}Yb_{0.2}F_3$ solid solution crystal show energy transfer processes between the subsystems of Tm^{3+} and Yb^{3+} ions: upconversion ($Yb^{3+} \rightarrow Tm^{3+}$) and downconversion ($Tm^{3+} \rightarrow Yb^{3+}$) luminescence.

It has been found that the intensities of upconversion luminescence lines with $\lambda_{em} = 347$ nm ($^1I_6 \rightarrow ^3F_4$) and 363 nm ($^1D_2 \rightarrow ^3H_6$) of Tm^{3+} ions depend on the excitation power in different ways. The time dependence of the first derivative of UC-luminescence intensity proved that population of the 1D_2 , 1G_4 , and 3H_4 energy levels of Tm^{3+} ions involves several energy transfer processes varying in the rate of luminescence rise.

The transient processes with duration of about 2 ms were detected in UC-luminescence kinetics of Tm^{3+} . Upon their completion the stable equilibrium states are established between the processes of population and spontaneous decay of the excited states of Tm^{3+} ions. As a result the time dependence of UC-luminescence

has a plateau. A conclusion has been made that these equilibrium states are possible under high-power excitation (more than 400 mW) with pulse duration $t_{ex} = (2.5-14)$ ms and modulation frequency $f_{mod} = 66.7$ Hz.

That way the investigation of UC-luminescence kinetics of crystals under rectangular pulse excitation with duration comparable with lifetime of excited energy levels of activator ions enables to detect the transient processes of energy transfer between two subsystems of rare earth ions.

This work was funded by the subsidy of the Russian Government (agreement # 02.A03.21.0002) to support the Program of Competitive Growth of Kazan Federal University among World's Leading Academic Centers and the subsidy allocated to Kazan Federal University for the state assignment in the sphere of scientific activities.

1. M. Wang, J.L. Liu, Y. X. Zhang, W. Hou, X. L. Wu, and S.K. Xu, *Mater. Lett.* **63**, 325 (2009).
2. Yu. Huang and C. M. Lieber, *Pure Appl. Chem.* **76**, 2051 (2004).
3. Q.-M. Huang, *Chinese J. Struct. Chem.* **29**, 993 (2010).
4. L. Zhenyu, Z. Kezhi, Z. Dan, L. Ning, and Q. Weiping, *J. Nanosci. Nanotechnol.* **11**, 9584 (2011).
5. A. Moadhen, C. Bouzidi, H. Elhouichet, R. Chtourou, and M. Oueslati, *Opt. Mat.* **31**, 1224 (2009).
6. R.S. Quimby, W.J. Miniscalco, and B. Thompson, *J. Appl. Phys.* **76**, 4472 (1994).
7. C. Chunyan, Q. Weiping, and Z. Jisen, *J. Nanosci. Nanotechnol.* **10**, 1900 (2010).
8. W. Guofeng, Q. Weiping, W. Lili, W. Guodong, Z. Peifen, and K. Ryongjin, *Opt. Express* **16**, 11907 (2008).
9. A. Cherif, A. Kanoun, and H. Maaref, *Optica Applicata* **41**, 235 (2011).